J. Coat. Technol. Res., **17** (1) 181–191, 2020
https://doi.org/10.1007/s11998-019-00256-9

A novel hydroxyl polyacrylate latex modified by OvPOSS and its application in two-component waterborne polyurethane coatings

Wu Zeng, Haowei Huang, Liujun Song, Xiang Jiang, Xinya Zhang

Abstract Octavinyl polyhedral oligomeric sisesquioxane (OvPOSS) was synthesized via hydrolysis and condensation of vinyltriethoxysilane. The structure of OvPOSS was determined by Fourier transform infrared spectroscopy (FTIR), X-ray diffraction (XRD), ^{1}H nuclear magnetic resonance and ^{29}Si nuclear magnetic resonance. A novel hydroxyl functional polyacrylate latex (HPA) with core–shell structure modified by OvPOSS (OvPOSS/HPA) was successfully prepared via emulsion copolymerization. Consequently two-component waterborne polyurethane (2K-WPU) coatings were prepared by using the as-prepared latex as hydroxyl components and hydrophilic polyisocyanates as curing agents. The structure and properties of OvPOSS/HPA were marked by FTIR, XRD, differential scanning calorimetry and thermogravimetric analysis. The results of FTIR and XRD show that OvPOSS has been successfully embedded into HPA, and OvPOSS occupies a homogeneous distribution in the HPA matrix. The effect of OvPOSS on the properties of OvPOSS/HPA as well as the application performance of 2K-WPU coatings film were also investigated. The results show that OvPOSS/HPA possesses core–shell structure with the OvPOSS core and enhanced thermal stability. The glass transition temperature (T_g) of OvPOSS/HPA with 2.0% OvPOSS content is 22.3°C, which is 8.4°C higher than that of pure HPA. The performance properties of the 2K-WPU coating films such as pencil hardness were also improved by incorporation of OvPOSS.

W. Zeng, H. Huang, L. Song, X. Jiang (✉),
X. Zhang (✉)
School of Chemistry and Chemical Engineering, South China University of Technology, Guangzhou 510641, China
e-mail: jiangx@scut.edu.cn

X. Zhang
e-mail: cexyzh@scut.edu.cn

Keywords Octavinyl polyhedral oligomeric silsesquioxane, Hydroxyl polyacylate latex, Core–shell structure, Two-component waterborne polyurethane coatings

Introduction

Polyurethane (PU) is becoming increasingly popular in many fields such as coatings,[1,2] foams,[3,4] adhesives,[5,6] 3D cell-laden bio-printing[7] and so on, owing to its excellent properties of good solvent and chemical resistance, abrasion resistance, hardness and flexibility, etc. Due to the increasingly strict legal requirements controlling the emission of volatile organic compounds (VOCs) and stronger demands for the thermosetting waterborne coatings to be of higher-performance and formaldehyde-free, one-component waterborne polyurethane (1K-WPU) coatings have attracted great attention over the past decade. However, because the high crosslinked WPU dispersion with high molecular weight is unstable in water, traditional 1K-WPU coatings possess a low molecular weight and low crosslinking density, which largely limits their extensive applications. Therefore, an increasing number of researchers are showing growing interests in developing two-component waterborne polyurethane (2K-WPU) coatings with improved properties.

Recently, many people have studied the synthesis of hydroxyl functional PU dispersions and waterborne polyisocyanate[8–10] preparation and reaction mechanism of 2K-WPU coatings.[11,12] One of the most important constituents for 2K-WPU coatings is hydroxyl functional acrylic polyols. Nabuurs[13] synthesized acrylic polymer latex and investigated the effect of the type and concentration of acid monomers on the properties of 2K-WPU coatings. Geurink[14] prepared a novel design of polyol binders by replacing carboxylate groups with sulfonate groups to avoid side reactions.

Wang[15] successfully prepared a type of high stable aqueous acrylic polyol dispersion by two-step acrylic acid addition and improved their compatibility with hydrophilic polyisocyanate binders. Moreover, due to the interesting properties of polysiloxane materials, such as low surface energy and high thermal stability, some researchers have begun to use siloxane modification to overcome the weakness of poor water and chemical resistance and to improve other properties of 2K-WPU coatings. The majority of recent papers focus on the synthesis of siloxane-modified 1K-WPU,[16–18] and few researchers have reported the investigation of 2K-WPU with siloxane modification. Zhang[19] prepared 2K-WPU coatings by using a silicone-modified acrylic latex by vinyltrimethoxysilane as the hydroxyl component, and hydrophilically-modified polyisocyanate as the curing agent. The results demonstrated that the hydroxyl value of the emulsion and the level of silicone monomer had an important effect on the properties of these coatings. Ge[20] synthesized a series of siloxane-modified 2K-WPU coatings with hydroxyl functional polyurethane aqueous dispersion modified by dihydroxylbutyl-terminated polydimethylsiloxane and hydrophilic-modified polyisocyanate. Compared with conventional 2K-WPU, the thermal stability of the siloxane-modified copolymers was greatly improved.

However, the hydrolysis and condensation of siloxane monomers readily occur in the aqueous phase, which severely affects the stability of hydroxyl functional latex, especially in the presence of large amounts of siloxane monomers. In addition, the reactivity of the C=C bond on siloxane monomers is not very high, resulting in low grafting efficiency of the siloxane, while the siloxane-modified films often show a phase separation structure due to the low surface energy and poor compatibility with other components[21,22]; thus, the domains in which siloxane aggregates usually have inferior performance. Therefore, some new silicone materials and modification methods are essential to develop the synthesis of a novel hydroxyl functional polyacryate latex.

Polyhedral oligomeric silsesquioxane (POSS) is a cage-type inorganic/organic hybrid molecule[23–25] possessing an inorganic core consisting of silicon and oxygen externally surrounded by nonreactive or reactive organic ligands. This unique structure can be expressed by a general formula $[(R\mathrm{SiO}_{3/2})n$, with $n = 8, 10, 12]$, where R represents a hydrogen atom or an organic functional group. A variety of organic–inorganic hybrid polymeric materials modified by mono-functional and multi-functional POSS have been prepared. Compared with unmodified polymers, the POSS-containing hybrid composites show improved performance such as low dielectric constant,[26,27] stronger mechanical properties,[28,29] enhanced thermal stability and elevated glass transition temperature (T_g),[30,31] oxidation resistance,[32–34] hydrophobicity,[35,36] and flammability resistance.[37] Octavinyl polyhedral oligomeric silsesquioxane (OvPOSS) with eight vinyl groups in different arms has been successfully incorporated into various polymer systems. Chen[38] reported a room-temperature vulcanized (RTV) silicone rubber with improved thermal stability, mechanical property and hardness using OvPOSS as crosslinking agents. Wang[39] synthesized a novel composite, OvPOSS-PS, with core–shell structure via batch emulsion polymerization, whose T_g and thermal stability were enhanced. Wang[33] prepared a UV-curable waterborne polyurethane acrylate (WPUA) modified by OvPOSS through photo-polymerization. The results showed that the WPUA/OvPOSS coatings possess better water resistance and thermal oxidative stability.

In this paper, a novel hydroxyl polyacrylate latex was synthesized by using OvPOSS as the functional monomer, and was applied to prepare 2K-WPU coatings with improved properties. We first synthesized OvPOSS by hydrolysis and condensation of vinyltriethoxysilane and OvPOSS/HPA by emulsion copolymerization. The 2K-WPU coatings were then prepared by using the as-prepared OvPOSS/HPA as the hydroxyl component and hydrophilic-modified polyisocyanate as the curing agent. The chemical structure, particle size distribution, surface morphology and thermal stability of OvPOSS and OvPOSS/HPA were characterized. The application properties, water and chemical resistance of 2K-WPU coatings were also investigated. It was found that OvPOSS has a positive effect on improving the hardness, thermal stability and water resistance properties of 2K-WPU coatings.

Experimental

Materials

Vinylethoxysilane (A151) was purchased from Foshan Daoning Chemical Reagent (China). Methanol and anhydrous alcohol (AR, 99.7%) was purchased from Tianjin Yongda Chemical Reagent (China). Commercial butyl acrylate (BA, 99%), methyl methacrylate (MMA), methacrylic acid (MAA, 99%) and 2-hydroxy propyl acrylate (2-HPA, 99%) were purified to remove the inhibitors before use. Potassium persulfate (KPS), sodium bicarbonate ($NaHCO_3$), sodium alkyl diphenyl ether disulfonate (DSB) and 2-acrylamide-2-methylpropanesulfonic acid (COPS-2) were offered by Aladdin Reagent Co., Ltd. (China). The hydrophilic-modified polyisocyanate curing agent is Bayhydur XP 2655 with –NCO content 21.2 ± 0.5% from Covestro (Germany).

Synthesis of octavinyl-POSS (OvPOSS)

The OvPOSS was synthesized by hydrolysis and condensation of vinyltriethoxysilane according to Scheme 1.[40] The general procedure is as follows: 105 mL of vinyltriethoxysilane was dissolved in

245 mL of anhydrous alcohol. Then, the pH of the reaction mixture was adjusted to 3 by hydrochloric acid. The system was allowed to react for 10 h at 60°C under N_2 and a white precipitation was generated. The white powder obtained from filtration was washed with cyclohexane and dried at 50°C in a vacuum drying oven. The final OvPOSS product was purified through recrystallization using tetrahydrofuran and methanol as a mixed solvent (volume ratio 1:3).

Synthesis of OvPOSS/HPA

The OvPOSS/HPA was synthesized via emulsion polymerization as shown in Scheme 2. The general preparation procedure is as follows: The reaction mixture of BA (19 g), MMA (22.5 g), MAA (1 g), 2-HPA (7.5 g) and OvPOSS (0.33 g) was well pre-mixed. Deionized water (50 g), $NaHCO_3$ (0.075 g), DSB (0.5 g) and COPS-2 (1 g) were charged into a four-necked flask with mechanical stirring and heated to 80°C. Then, the KPS solution (0.25 g KPS dissolved in 11 g deionized water) as an initiator was added. Then, 10% of the reaction mixture as seed monomer was fed dropwise into the flask within 15 min under continuous stirring. The system temperature was kept at 80–82°C for 20 min after the seed monomer addition finished, and then the rest of monomer mixture was fed into the reaction system for 3 h. The reactants were stirred for another 1 h at 80–82°C when the feeding was completed. At the end of the reaction, the latex was filtered through a 200-mesh sieve. The amount of OvPOSS added varied from 0% to 2% of the mass of the acrylate monomer. For comparison, the pure HPA was also prepared by the same process without OvPOSS.

Preparation of 2K-WPU coatings

OvPOSS/HPA with a set mass was placed in a beaker, and the curing agent XP 2655 with a calculated amount was added to the beaker and stirred fully for even mixing. Then, the prepared 2K-WPU coatings were coated onto clean glass panels and cured at room temperature for the full evaporation of the water and the crosslinking reaction. The thickness of the wet film was 120 μm. Finally, the 2K-WPU coatings films were dried further in a vacuum oven at 50°C for 24 h. A series of 2K-WPU coatings films were prepared by OvPOSS/HPA with different amounts of OvPOSS and

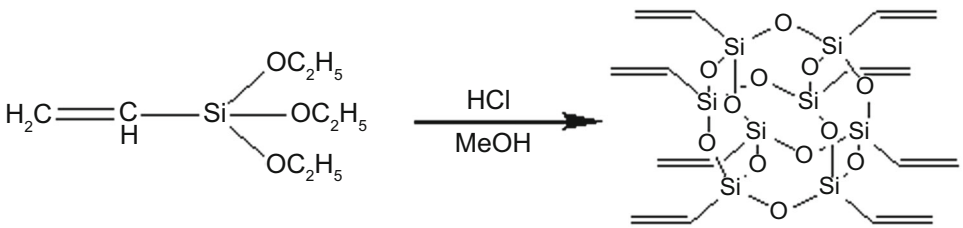

Scheme 1: The synthetic route of OvPOSS

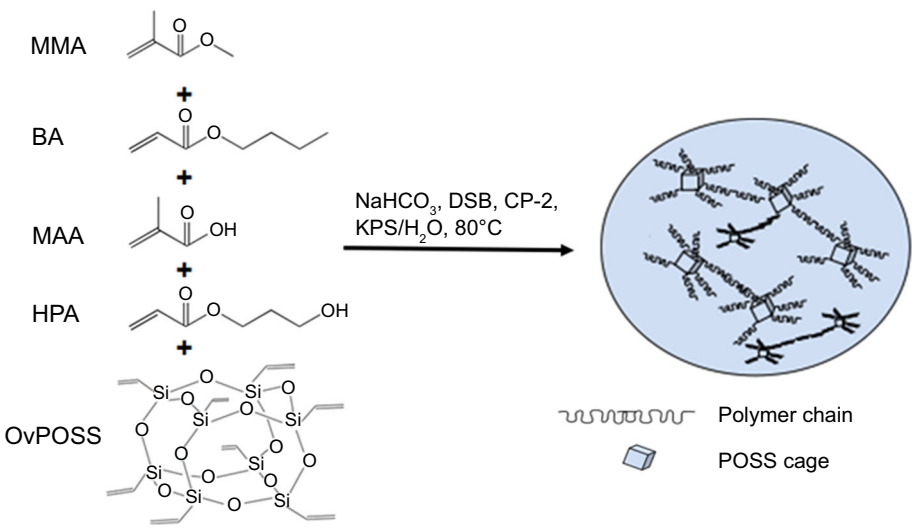

Scheme 2: The synthetic route of OvPOSS/HPA

XP 2655 with the constant NCO/OH molar ratio of 1.5:1.

Characterizations and instruments

Nuclear magnetic resonance (NMR) The ^{1}H NMR and ^{29}Si NMR measurements were conducted on a Bruker AVAVXE 300 spectrometer (Swiss) at room temperature. Deuterated chloroform was used as the solvent.

Dynamic light scattering (DLS) The latex particle size and its distribution were determined with a granularity analyzer (ZS Nano S) from Malvern (UK).

X-ray diffraction (XRD) XRD was carried out by a Bruker D8 ADVANCE diffractometer (Swiss) with Cu Kα radiation (λ = 0.15418) at a scanning rate of 0.01°/s.

Transmission electron microscopy (TEM) TEM images were measured using a HITACHI H-7650 instrument (Japan), conducting an accelerating voltage of 80 kV.

Fourier transform infrared (FTIR) FTIR spectra of the samples were recorded between 4000 and 400 cm^{-1} by a Spectnlm2000 spectrometer (USA).

Scanning electron microscope (SEM) SEM micrographs were investigated with a Nova NANOSEM 430 (USA), and an energy dispersive X-ray spectrometer (EDS) was linked to the SEM, operating at 10 kV.

Thermogravimetric analysis (TGA) TGA was carried out with a NETZSCH TG 209 thermo-analyzer instrument (Germany) in a temperature range of room temperature to 600° under N_2 atmosphere at a heating rate of 10°C/min.

Differential scanning calorimetry (DSC) DSC analysis was detected by a NETZSCH DSC204 (Germany). The scan rate was 10°C/min within the temperature range of −20 to 120°C at N_2 atmosphere.

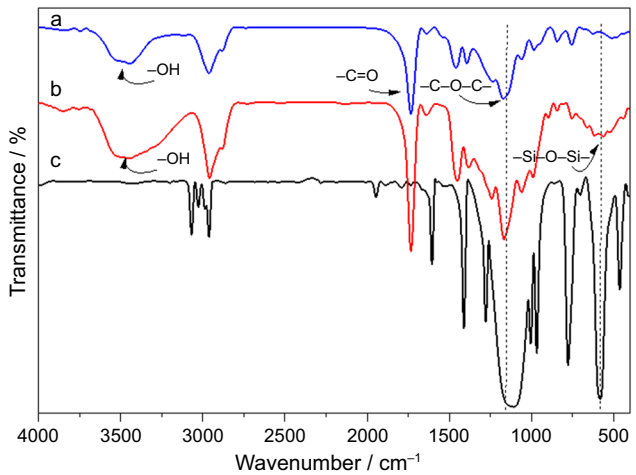

Fig. 1: FTIR spectra of pure HPA (a), 1.0% OvPOSS/HPA (b) and OvPOSS (c)

Results and discussion

Structure characterization of OvPOSS

OvPOSS was synthesized via hydrolytic condensation of vinyltriethoxysilane. The FTIR spectra of Fig. 1 are of (a) pure HPA, (b) 1.0 wt% OvPOSS/HPA and (c) OvPOSS, respectively. As Fig. 1c shows, the molecular structure of OvPOSS is simple but highly symmetrical, and each peak in the infrared spectrum is very visible and independent. The strong absorption band at 1101 cm^{-1} is attributed to the antisymmetric stretching vibration of Si–O–Si from the POSS cage, while the band at 586 cm^{-1} is due to the symmetric vibration of Si–O–Si. The absorption peaks of 777 and 1605 cm^{-1} are assigned to the stretching vibration of the Si–C and C=C double bond. The absorption peaks at 3072, 2960 cm^{-1} [υ (C–H)], 1412, and 1278 cm^{-1}[δ (C–H)] are the stretch and deformation vibration peaks of the

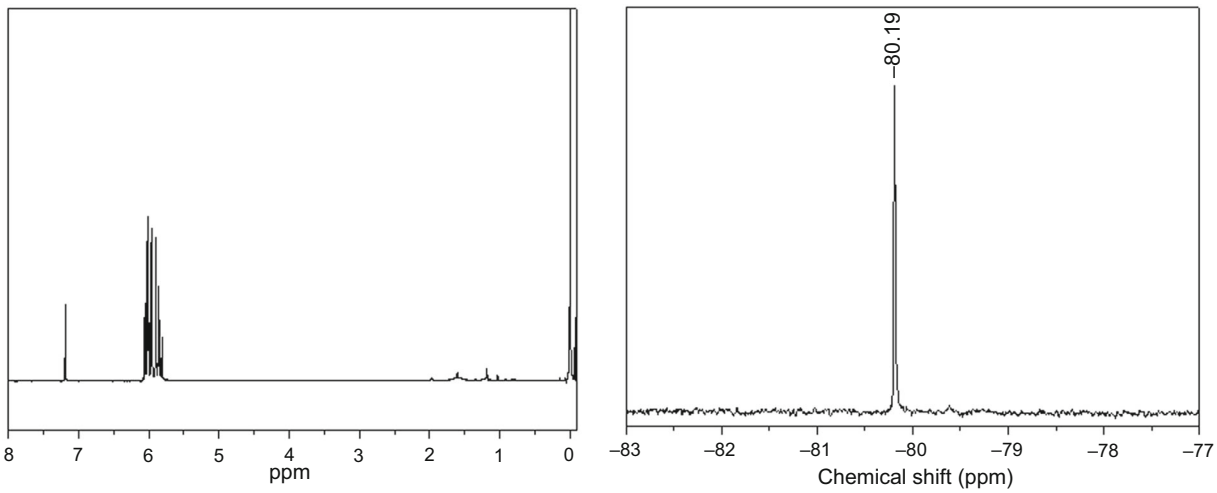

Fig. 2: ^{1}H NMR and ^{29}Si NMR spectra of OvPOSS

C–H bonds of Si–CH=CH_2. However, the characteristic peak of Si–OH between 880 and 830 cm^{-1} does not appear, indicating that the resultant OvPOSS was the product of complete hydrolysis. All these characteristic peaks prove that the desired OvPOSS was obtained.

The ^{1}H NMR and ^{29}Si NMR analyses for OvPOSS were carried out with $CDCl_3$ as solvent. The spectra of ^{1}H NMR and ^{29}Si NMR spectra are shown in Fig. 2. In Fig. 2a, the multiple peaks at 5.81–6.06 ppm are attributed to the proton on the vinyl groups of OvPOSS, in which the corresponding peak area ratio is 43:79 (almost 1:2), corresponding to the two protons on the vinyl group. Multiple splitting peaks are due to spin-coupling effects between multiple H atoms in different chemical environments. For the ^{29}Si NMR spectrum in Fig. 2b, there is only one resonance absorption peak, at − 80.19 ppm, indicating that all the obtained Si atoms are all in the same chemical environment. According to previously reported references (40) and (41), OvPOSS has a cage symmetry structure, and there is only one silicon atom in the molecule. Therefore, both FTIR and NMR results confirm that the desired OvPOSS was obtained.

In order to further confirm that POSS with eight vinyl groups was obtained, the XRD characterization was conducted, as displayed in Fig. 3, where the XRD pattern of the pure OvPOSS is in Fig. 3a. The OvPOSS of Fig. 3a shows several strong diffraction peaks at 2θ's of 9.7°, 13.0°, 19.5°, 20.9°, 22.8°, and 23.5°. These values are representative for the crystal structure of OvPOSS.[34]

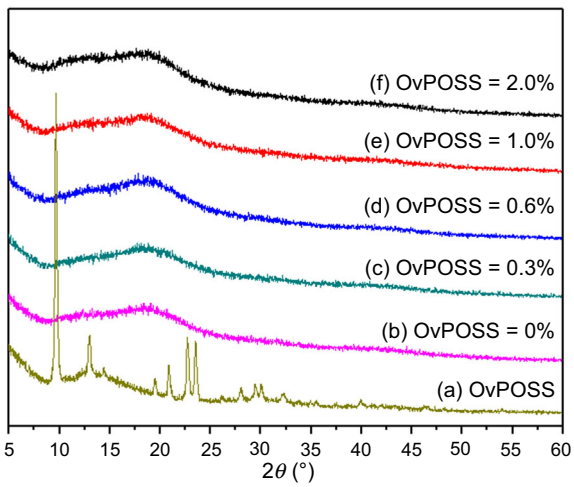

Fig. 3: XRD patterns of the pure OvPOSS, and OvPOSS/HPA

Structure characterization of OvPOSS/HPA

The OvPOSS/HPA prepared by emulsion polymerization is illustrated in Scheme 2. The FTIR spectra of Figs. 1a and 1b are the FTIR spectra of pure HPA and 1.0 wt% OvPOSS/HPA, respectively. From Fig. 1a, the band at 3520 cm^{-1} is attributed to the non-hydrogen-bonded OH groups and the band at 3450 cm^{-1} is caused by hydrogen bonding of OH groups, shifting to lower frequencies. Due to the high content of OH groups in HPA, the two bands at 3450 and 3520 cm^{-1} have a tendency to overlap. The characteristic stretching peaks of $–CH_3$ and $–CH_2$ groups are at 2955 and 2874 cm^{-1}, respectively. A strong absorption peak at 1731 cm^{-1} belongs to the C=O groups while the stretching vibration at 1170 cm^{-1} is assigned to the C–O–C groups or Si–O–Si groups. Compared with the spectrum of pure HPA, the absorption band at 1170 cm^{-1} from the C=O group becomes sharp and strong in Fig. 1b when OvPOSS is copolymerized with acrylates to achieve OvPOSS/HPA. And meanwhile, a new band at 585 cm^{-1} corresponding to the Si–O–Si bending band is presented. The results of FTIR show that OvPOSS was successfully introduced into the main chain of HPA.

Furthermore, in order to investigate the distribution of OvPOSS in OvPOSS/HPA, the XRD patterns of OvPOSS/HPA with different contents of 0.0, 0.3, 0.6,

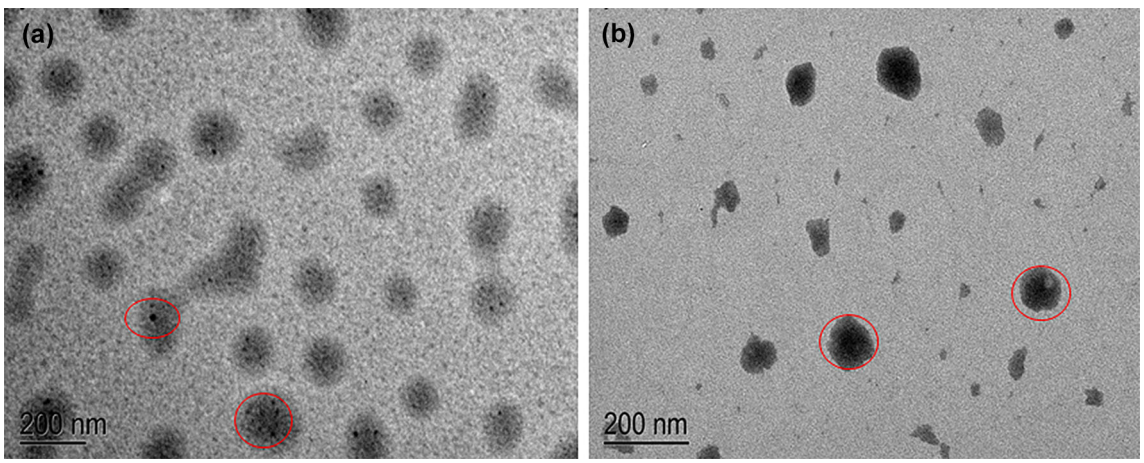

Fig. 4: TEM morphology of OvPOSS/HPA hybrid particles with 0.6% OvPOSS (a) and 2.0% OvPOSS

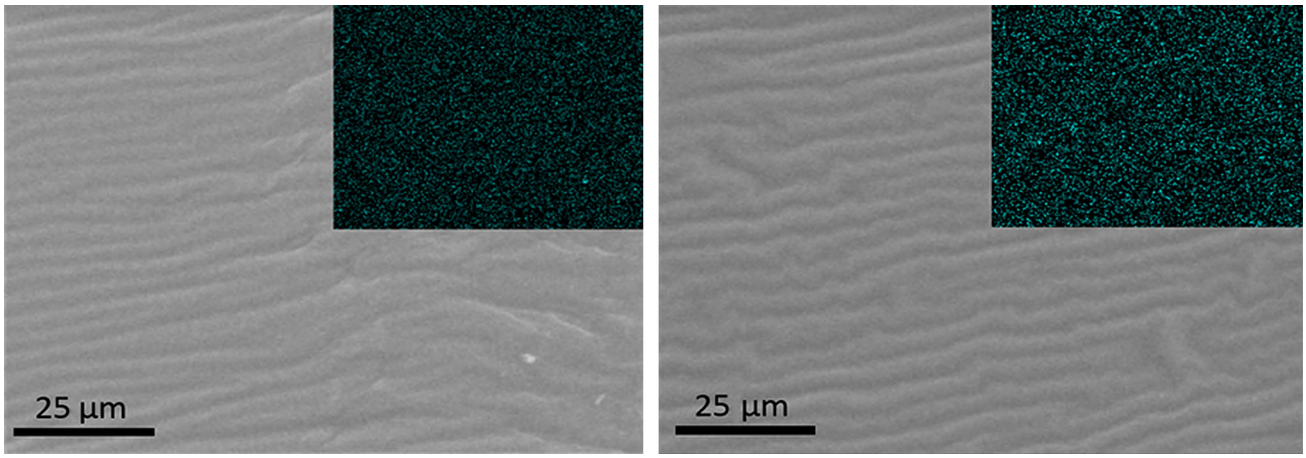

Fig. 5: SEM and Si EDS mapping micrographs of the cross-section of 2.0 wt% OvPOSS/HPA

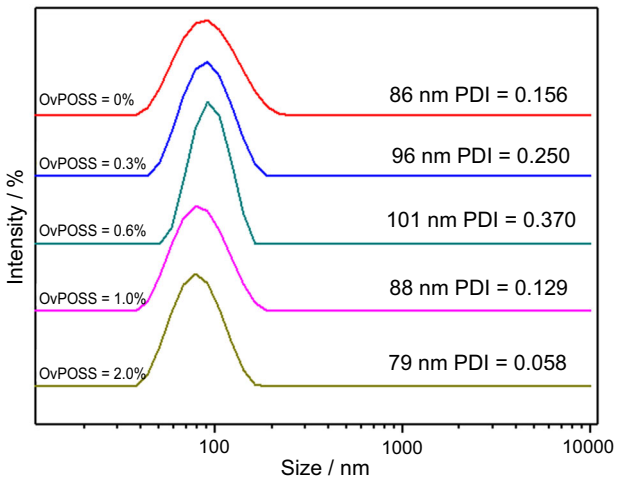

Fig. 6: Particle size distribution of HPA and OvPOSS/HPA with different amounts of OvPOSS: (a) 0.0%; (b) 0.3%; (c) 0.6%; (d) 1.0%; (e) 2.0%

1.0 and 2.0 wt% were employed, as shown in Figs. 3b–3f. We know that the main characteristic crystal diffraction peaks of OvPOSS in 2θ are always presented at 9.7°, 19.5° and 22.8°. From Figs. 3b–3f, all the OvPOSS characteristic diffraction peaks disappeared, and all the OvPOSS/HPA showed similar wide-angle X-ray diffraction patterns to pure HPA (0.0 wt% OvPOSS sample), which suggests that all OvPOSS are incorporated in the HPA main chain homogeneously and no significant micro-phase separation has occurred.

In order to observe the clear morphology of OvPOSS/HPA, Its morphology was characterized by TEM as shown in Fig. 4, wherein OvPOSS/HPA hybrid particles with 0.6% OvPOSS (a) and 2.0% OvPOSS (b), respectively. It is obvious that the OvPOSS/HPA possesses a core–shell structure and the latex particles are of about 100 nm, and the OvPOSS are uniformly distributed in the polymer matrix and surrounded by polyacrylate homo-polymer shell. In Fig. 4a, the black dots in the latex particles are the OvPOSS domains due to the denser electronic cloud density of OvPOSS and higher crosslinking degree of OvPOSS/HPA. With the higher OvPOSS contents (2.0 wt%) in Fig. 4b, the black domains of OvPOSS in the latex particle centers are larger and darker, and the morphology of the OvPOSS/HPA has changed from regular to irregular with smaller particle sizes but yet a core–shell structure.

In addition, the SEM micrographs of the cross-sections of OvPOSS/HPA and Si EDS mappings (Fig. 5; OvPOSS/HPA hybrid particles with (a) 0.6 wt% OvPOSS and (b) 2.0 wt% OvPOSS) also show that OvPOSS are distributed homogeneously in the HPA matrix and no obvious phase separation is observed at a micrometric scale among all the samples. These results are consistent with the illustration of XRD in Fig. 3.

Particle size distribution of OvPOSS/HPA

Figure 6 shows the particle size distribution of the pure HPA and OvPOSS/HPA. The average diameter of pure HPA particles (Fig. 6a) is 86 nm. With 0.3 and 0.6 wt% OvPOSS incorporated into the HPA, the diameters of the OvPOSS/HPA (Figs. 6b and 6c) are 96 and 101 nm, which are larger than that of pure HPA. This is probably attributed to the incorporation of POSS cages. When the OvPOSS are copolymerized with acrylate monomers, the acrylate monomers are first grafted onto the eight vinyl groups in the OvPOSS and particles with OvPOSS as core-formed. After all the OvPOSS were exhausted, the residual acrylate monomers further continue copolymerizing with the core particles to form the shell polymer based on the polyacrylate chain. As a result, the size of OvPOSS/HPA gradually increased and the distribution became wider. However, when the amount of OvPOSS reachOvPOSS wt% or even 2.0 wt% (Figs. 6d and 6e), the average diameters of HPA decrease to 88 and 79 nm, and the PDIs decrease to

0.129 and 0.058. The possible reasons for the decrease of particle size are as follows: the steric effect was produced by a large number of OvPOSS molecules during emulsion polymerization, which shortens the chain length of grafted polyacrylate molecules in the post-reaction stage, and consequently shortens the chain length of the shell polyacrylate molecules as well as the particle size of the latex particles. The more OvPOSS involved in the reaction, the stronger the steric hindrance effect. On the other hand, according to relevant literature reports,[30,42] OvPOSS molecules promote the crosslinking between molecular chains when they form crosslinked products, so as to produce more compact particles. Therefore, when the amount of OvPOSS further increases, the particle size of the hybrid latex particles decreases as a consequence.

Thermal properties of OvPOSS/HPA films

Glass transition behavior

The glass transition temperature of all the samples with various OvPOSS contents was measured by DSC as shown in Fig. 7, while the T_g for the OvPOSS/HPA with various OvPOSS contents are listed in Table 1. It is clearly demonstrated that the T_g of all the OvPOSS/HPA are higher than that of the pure HPA of 13.9°C. The T_g of the OvPOSS/HPA rises with the increasing OvPOSS contents. The T_g of 2.0% OvPOSS/HPA latex reaches 22.3°C, which is 8.4°C higher than that of pure HPA.

According to the literature reports,[43–45] the crosslinking effect, steric hindrance and dipole–dipole interaction of OvPOSS have an important impact on the thermal properties of nano-composite materials with the modification of OvPOSS. For this as-prepared OvPOSS/HPA, the incorporation of OvPOSS obviously increases the T_g of OvPOSS/HPA. We analyze possible reasons as follows: on the one hand, the OvPOSS cage structure leads to a strong space steric effect, which limits the movement of the hydroxyl polyacrylate molecular chain. On the other hand, since the OvPOSS/HPA particles contain OvPOSS molecules, its Si–O–Si bond also promotes the improvement of the T_g of OvPOSS/HPA. And, meanwhile, when OvPOSS is copolymerized with acrylate monomers, the OvPOSS/HPA would form a crosslinking network due to the OvPOSS's special eight vinyl groups in different arms, which also restricts the chain movement

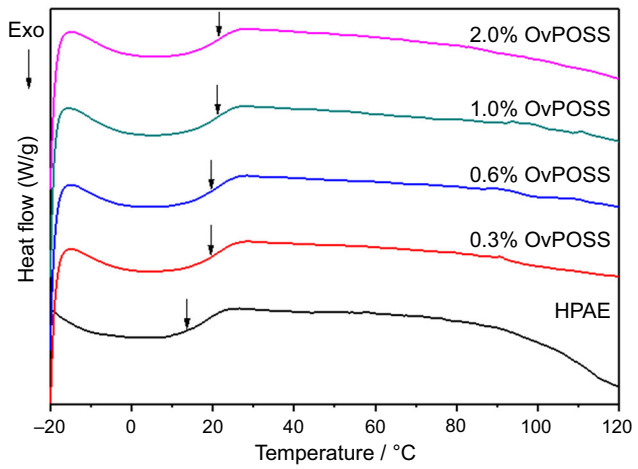

Fig. 7: DSC curves of pure HPA and OvPOSS/HPA

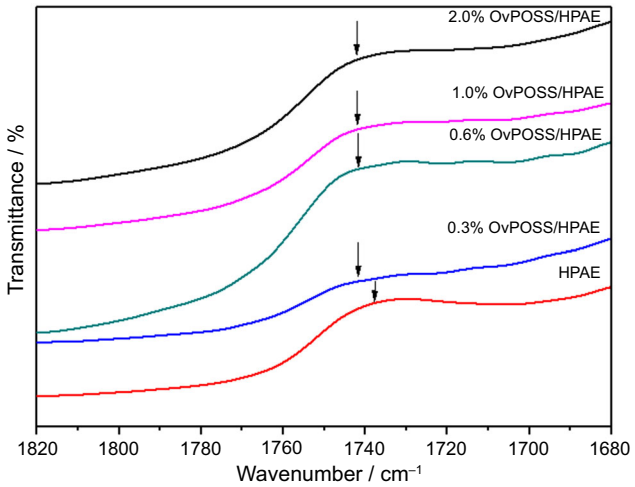

Fig. 8: Expanded FTIR spectra in the region from 1820 cm^{-1} to 1620 cm^{-1} of pure HPA and OvPOSS/HPA

Table 1: Thermal properties of HPA with different OvPOSS contents

Sample	T_g (°C)	T^a_{dec1} (°C)	T^b_{dec2} (°C)	T^c_{max} (°C)	R^d (%)
0.0%OvPOSS	13.9	282.9	334.9	398.9	0
0.3%OvPOSS	19.7	283.1	335.1	399.0	0.3
0.6%OvPOSS	19.8	306.3	348.3	398.2	2.8
1.0%OvPOSS	21.6	288.8	335.3	398.4	1.9
2.0%OvPOSS	22.3	299.3	339.3	396.9	3.3

[a]Thermal decomposition temperature of 5% weight loss

[b]Thermal decomposition temperature of 10% weight loss

[c]Thermal decomposition temperature of the maximum weight loss

[d]Residue at 600°C

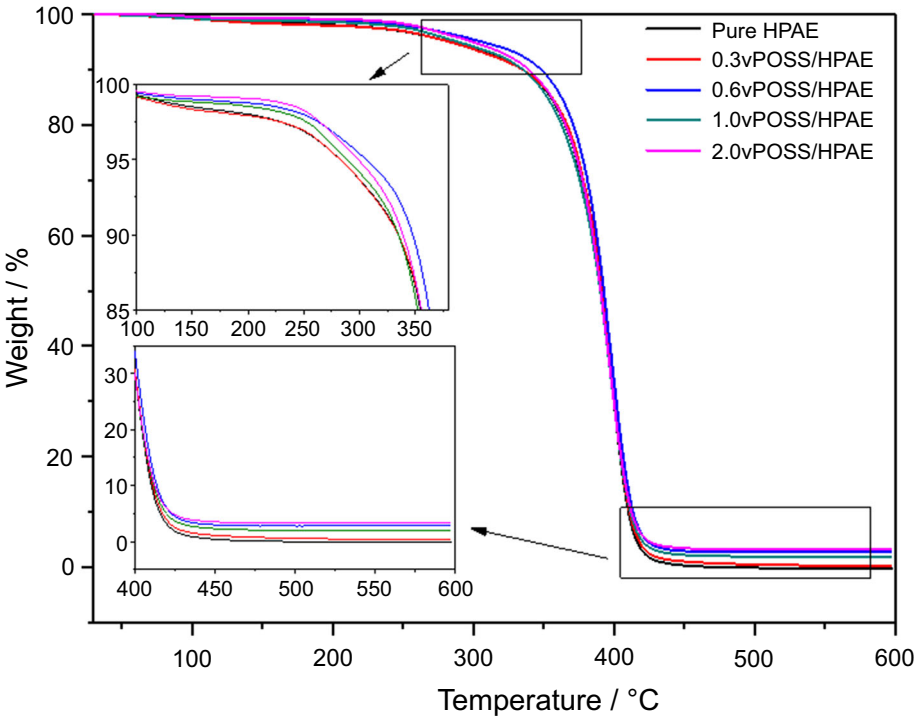

Fig. 9: TGA curves of pure HPA and OvPOSS/HPA

and the activity of polymer chain segments in the polymer and thus leads to an increasing T_g.

In addition to the POSS crosslinking effect, the dipole–dipole interaction between acrylate polymer chains and OvPOSS cores may be another important reason to increase the T_g of OvPOSS/HPA. To clearly understand the effect of dipole–dipole interaction on T_g enhancement, the FTIR spectra was carefully investigated. The enlarged FTIR spectra of various OvPOSS/HPA and the pure HPA ranging from 1820 to 1680 cm^{-1} are shown in Fig. 8. The pure HPA has a characteristic carbonyl vibration band located at 1731 cm^{-1}. When HPA is modified with 0.3 wt% OvPOSS, the carbonyl absorption begins to shift from 1731 to 1741 cm^{-1}. There is a trend that the carbonyl absorption peak moves towards higher wavenumbers when more OvPOSS are incorporated into the HPA. This indicates that, in these OvPOSS/HPA hybrid composites, the dipole distance between the OvPOSS molecules and the acrylate polymer decreases while dipole–dipole interactions between acrylate polymer chains and OvPOSS increase. Therefore, in addition to the steric hindrance effect and crosslinking structure, the dipole–dipole interaction further restricts the HPA polymer chain mobility and yields a positive contribution to the T_g enhancement of the hybrid composites.

Thermal stability TGA

Figure 9 depicts the thermal stability of pure HPA and OvPOSS/HPA under nitrogen condition. The initial thermal decomposition temperatures and char yields for different samples are shown in Table 1. All the samples displayed similar degradation steps in the TGA curves, which suggested that the existence of OvPOSS did not significantly change the degradation mechanism of the hybrid composites. More interestingly, the T_{dec1} and T_{dec2} (5.0% and 10.0% mass loss temperatures) were increased by 23.4 and 13.4°C, respectively, for the composites with OvPOSS ranging from 0% to 0.6%. These results suggest that incorporation of OvPOSS increases both T_{dec} and the char yield. This fact indicates that the thermal stability of HPA can be improved by OvPOSS.

Properties of 2K-WPU coatings

The SEM morphology of 2K-WPU coatings using the as-prepared OvPOSS/HPA as the hydroxyl component and hydrophilic-modified polyisocyanate as the curing agent are shown in Fig. 10. The modified 2K-WPU coatings film is similar to the film prepared by pure HPA, which signifies that the introduction of OvPOSS does not weaken the compatibility between the HPA and polyisocyanate. In addition, OvPOSS has a low surface energy and is easy to introduce to the surface of the 2K-WPU coatings film. Consequently, a rougher surface film is presented.

Table 2 shows the application properties of 2K-WPU coating films with gradient contents of OvPOSS. It is obvious that the film performances of all these samples satisfy practical applications. The addition of

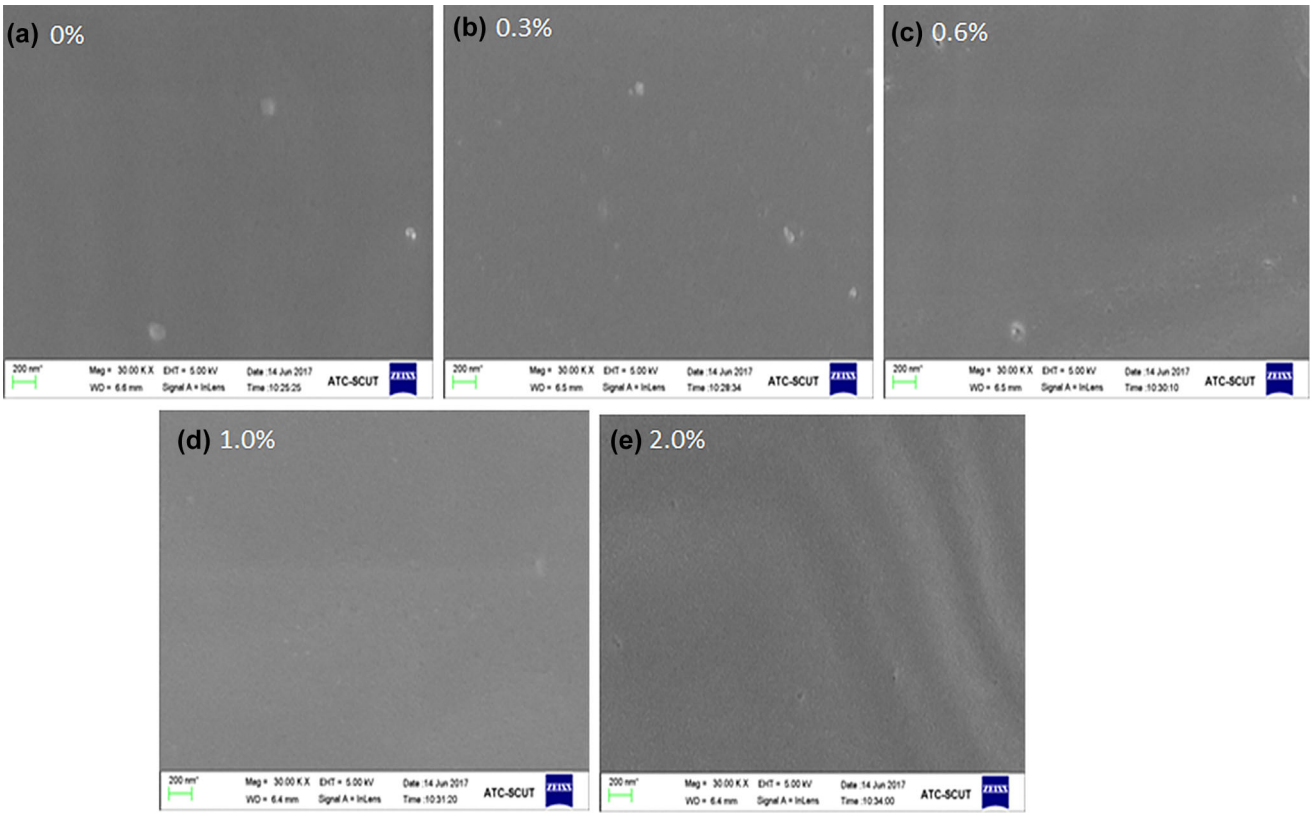

Fig. 10: SEM photographs of 2K-WPU coatings with different amounts of OvPOSS: (a) 0.0 wt%; (b) 0.3 wt%; (c) 0.6 wt%; (d) 1.0 wt%; (e) 2.0 wt%

Table 2: Effect of OvPOSS content on the properties of 2K-WPU coatings

OvPOSS (wt%)	0.0	0.3	0.6	1.0	2.0
Compatibility test	Pass	Pass	Pass	Pass	Pass
Appearance	Smooth, flat, transparent	Smooth, flat, transparent	Smooth, flat, transparent	Smooth, flat, transparent	Smooth, flat, transparent
Pencil hardness	H	H	3H	3H	2H
Gloss (60°)	87.8	95.4	99.5	110.9	87.4
Adhesion on cross-hatching	1	1	1	1	2
Chemical resistance (24 h)					
Acid, 10% H_2SO_4 spot	Pass	Pass	Pass	Pass	Pass
Acid, 10% HCl spot	Pass	Pass	Pass	Pass	Pass
Acid, 10% acetic acid spot	Pass	Pass	Pass	Pass	Pass
Base, 10% NaOH spot	Pass	Pass	Pass	Pass	Pass
Acetone spot	Pass	Pass	Pass	Pass	Pass
Xylene spot	Pass	Pass	Pass	Pass	Pass
Ethanol spot	Pass	Pass	Pass	Pass	Pass

OvPOSS did not change the compatibility and appearance of the coatings, but the pencil hardness of the 2K-WPU coatings film is significantly improved, which results from the highly crosslinked siloxane cage structure. What is more, the gloss of the OvPOSS-modified 2K-WPU film is increased. This is probably due to the smaller size of the OvPOSS-modified hydroxyl acrylate latex particles, as shown in Fig. 7.

The OH groups in smaller particles are easier to contact and react with NCO groups in polyisocyanate. The depression of 2 wt% OvPOSS on the hardness and gloss properties may be related to the bulk existence of overloaded OvPOSS, which has a steric hindrance which can damage the complete reaction with the NCO groups.

Conclusions

A novel hydroxyl functional acrylic latex modified by OvPOSS (OvPOSS/HPA) has been successfully developed by emulsion copolymerization. The FTIR spectra indicate that OvPOSS has been successfully embedded into the HPA latex and the XRD pattern and EIS mappings results imply that OvPOSS molecules were distributed homogeneously. The OvPOSS/HPA latex displays a clear core–shell structure. Compared with pure HPA, the average diameter of OvPOSS/HPA increases to 100.8 nm (0.6 wt% OvPOSS/HPA), but then decreases as the amount of OvPOSS increases. The incorporation of OvPOSS improves T_g and the thermal stability of OvPOSS/HPA. When the content of OvPOSS is 2.0 wt%, the T_g of OvPOSS/HPA is 22.3°C, which is 8.4°C higher than that of pure HPA. The properties of the 2K-WPU coatings film prepared by OvPOSS/HPA and hydrophilic polyisocyanates, such as hardness, and water and chemical resistance, are improved. These results demonstrate that the presence of OvPOSS obviously enhanced the properties of 2K-WPU coatings.

Acknowledgments The authors gratefully acknowledge the financial support of the Science and Technology Planning Project of Guangzhou Science Technology & Innovation Commission (Grant No. 201607010049) and the Science and Technology Planning Project of Guangdong Province, China (2015A010105008).

References

1. Deng, YJ, Zhou, C, Zhang, MY, Zhang, HX, ''Effects of the Reagent Ratio on the Properties of Waterborne Polyurethanes-Acrylate for Application in Damping Coating.'' *Prog. Org. Coat.*, **122** 239–247 (2018)
2. Yousefi, E, Ghadimi, MR, Amirpoor, S, Dolad, A, ''Preparation of New Superhydrophobic and Highly Oleophobic Polyurethane Coating with Enhanced Mechanical Durability.'' *Appl. Surf. Sci.*, **454** 201–209 (2018)
3. Hu, T, Xuan, SH, Ding, L, Gong, XL, ''Stretchable and Magneto-Sensitive Strain Sensor Based on Silver Nanowire-Polyurethane Sponge Enhanced Magnetorheological Elastomer.'' *Mater. Design*, **156** 528–537 (2018)
4. Prociak, A, Kuranska, M, Cabulis, U, Ryszkowska, J, Leszczynska, M, Uram, K, Kirpluks, M, ''Effect of Bio-polyols with Different Chemical Structures on Foaming of Polyurethane Systems and Foam Properties.'' *Ind. Crops Prod.*, **120** 262–270 (2018)
5. Hausberger, A, Major, Z, Theiler, G, Gradt, T, ''Observation of the Adhesive- and Deformation-Contribution to the Friction and Wear Behaviour of Thermoplastic Polyurethanes.'' *Wear*, **412** 14–22 (2018)
6. Akram, N, Zia, KM, Saeed, M, Mansha, A, Khan, WG, ''Morphological Studies of Polyurethane Based Pressure Sensitive Adhesives by Tapping Mode Atomic Force Microscopy.'' *J. Polym. Res.*, **25** (9) 193–203 (2018)
7. Hsiao, SH, Hsu, SH, ''Synthesis and Characterization of Dual Stimuli-Sensitive Biodegradable Polyurethane Soft Hydrogels for 3D Cell-Laden Bioprinting.'' *ACS Appl. Mater. Inter.*, (2018). https://doi.org/10.1021/acsami.8b08362
8. Guo, L, Huang, S, Qu, JQ, ''Synthesis and Properties of High-Functionality Hydroxyl-Terminated Polyurethane Dispersions.'' *Prog. Org. Coat.*, **119** 214–220 (2018)
9. Xu, W, Zhao, WJ, Hao, LF, Wang, S, Pei, M, Wang, XC, ''Synthesis and Characterization of Novel Fluoroalkyl-Terminated Hyperbranched Polyurethane Latex.'' *Appl. Surf. Sci.*, **436** 1104–1112 (2018)
10. Zhu, ZW, Li, RQ, Zhang, CY, Gong, XL, ''Preparation and Properties of High Solid Content and Low Viscosity Waterborne Polyurethane-Acrylate Emulsion with a Reactive Emulsifier.'' *Polymers*, **10** (2) 154 (2018)
11. Chai, CP, Hou, JH, Yang, XH, Ge, Z, Huang, MH, Li, GP, ''Two-Component Waterborne Polyurethane: Curing Process Study Using Dynamic In Situ IR Spectroscopy.'' *Polym. Test*, **69** 259–265 (2018)
12. Wu, GM, Liu, GG, Chen, J, Kong, ZW, ''Preparation and Properties of Thermoset Composite Films from Two-Component Waterborne Polyurethane with Low Loading Level Nanofibrillated Cellulose.'' *Prog. Org. Coat.*, **106** 170–176 (2017)
13. Nabuurs, T, Pears, D, Overbeek, A, ''Defect-Free Coatings from Two-Pack Isocyanate Curable Acrylic Dispersions.'' *Prog. Org. Coat.*, **35** 129–140 (1999)
14. Geurink, PJA, Scherer, T, Buter, R, Steenbergen, A, Henderiks, H, ''A Complete New Design for Waterborne 2-Pack PUR Coatings with Robust Application Properties.'' *Prog. Org. Coat.*, **55** 119–127 (2006)
15. Wang, L, Xu, F, Li, H, Liu, Y, Liu, Y, ''Preparation and Stability of Aqueous Acrylic Polyol Dispersions for Two-Component Waterborne Polyurethane.'' *J. Coat. Technol. Res.*, **14** 1–9 (2017)
16. Suen, MC, Gu, JH, Hwang, JJ, Wu, CL, Lee, HT, ''In-Situ Polymerization and Characteristic Properties of the Waterborne Poly(siloxanes-urethane)s Nanocomposites Containing Graphene.'' *J. Polym. Res.*, **25** (1) 32–46 (2018)
17. Oguz, O, Simsek, E, Soz, CK, Heinz, OK, Yilgor, E, Yilgor, I, Menceloglu, YZ, ''Effect of Filler Content on the Structure-Property Behavior of Poly(ethylene oxide) Based Polyurethaneurea-Silica Nanocomposites.'' *Polym. Eng. Sci.*, **58** (7) 1097–1107 (2018)
18. Li, Q, Guo, LH, Qiu, T, Ye, J, He, LF, Li, XY, Tuo, XL, ''Polyurethane/Polyphenylsilsequiloxane Nanocomposite: from Waterborne Dispersions to Coating Films.'' *Prog. Org. Coat.*, **122** 19–29 (2018)
19. Zhang, FA, Yu, CL, ''Application of a Silicone-Modified Acrylic Emulsion in Two-Component Waterborne Polyurethane Coatings.'' *J. Coat. Technol. Res.*, **4** 289–294 (2007)
20. Ge, Z, Luo, Y, ''Synthesis and Characterization of Siloxane-Modified Two-Component Waterborne Polyurethane.'' *Prog. Org. Coat.*, **76** 1522–1526 (2013)

21. Majumdar, P, Webster, DC, ''Influence of Solvent Composition and Degree of Reaction on the Formation of Surface Microtopography in a Thermoset Siloxane–Urethane System.'' *Polymer*, **47** 4172–4181 (2006)
22. Majumdar, P, Webster, DC, ''Surface Microtopography in Siloxane–Polyurethane Thermosets: the Influence of Siloxane and Extent of Reaction.'' *Polymer*, **48** 7499–7509 (2007)
23. Li, YC, Luo, CH, Li, XH, Zhang, KQ, Zhao, YH, Zhu, KY, Yuan, XY, ''Submicron/Nano-Structured Icephobic Surfaces Made from Fluorinated Polymethylsiloxane and Octavinyl-POSS.'' *Appl. Surf. Sci.*, **360** 113–120 (2016)
24. Tao, C, Li, XH, Liu, B, Zhang, KQ, Zhao, YH, Zhu, KY, Yuan, XY, ''Highly Icephobic Properties on Slippery Surfaces Formed from Polysiloxane and Fluorinated POSS.'' *Prog. Org. Coat.*, **103** 48–59 (2017)
25. Liu, N, Yu, JY, Meng, YY, Liu, YZ, ''Hyperbranched Polysiloxanes Based on Polyhedral Oligomeric Silsesquioxane Cages with Ultra-High Molecular Weight and Structural Tuneability.'' *Polymers*, **10** (5) 495–508 (2018)
26. Ke, F, Zhang, C, Guang, S, Xu, H, ''POSS Core Star-Shape Molecular Hybrid Materials: Effect of the Chain Length and POSS Content on Dielectric Properties.'' *J. Appl. Polym. Sci.*, **127** 2628–2634 (2012)
27. Du, BX, Su, JG, Tian, M, Han, T, Li, J, ''Understanding Trap Effects on Electrical Treeing Phenomena in EPDM/POSS Composites.'' *Sci. Rep.*, **8** 1 (2018). https://doi.org/10.1038/s41598-018-26773-y
28. Hou, GX, Li, N, Han, HZ, Huo, L, Gao, JG, ''Hybrid Cationic Ring-Opening Polymerization of Epoxy Resin/Glycidyloxypropyl-Polyhedral Oligomeric Silsesquioxane Nanocomposites and Dynamic Mechanical Properties.'' *Iran. Polym. J.*, **24** (4) 299–307 (2015)
29. Zhuo, YZ, Hakonsen, V, He, ZW, Xiao, SB, He, JY, Zhang, ZL, ''Enhancing the Mechanical Durability of Icephobic Surfaces by Introducing Autonomous Self-Healing Function.'' *ACS Appl. Mater. Inter.*, **10** (14) 11972–11978 (2018)
30. Liao, WB, Huang, XX, Ye, LY, Lan, SH, Fan, HB, ''Synthesis of Composite Latexes of Polyhedral Oligomeric Silsesquioxane and Fluorine Containing Poly(styrene-acrylate) by Emulsion Copolymerization.'' *J. Appl. Polym. Sci.*, **133** (21) 43455–43460 (2016)
31. Chen, SH, Gao, JG, Han, HZ, Wang, C, ''Mechanical and Thermal Properties of Epoxy-POSS Reinforced(biphenyl Diol Formaldehyde/Epoxy Hybrid Resin) Composites.'' *Iran. Polym. J.*, **23** (8) 609–617 (2014)
32. Yu, CY, Wan, HQ, Chen, L, Li, HX, Cui, HX, Ju, PF, Zhou, HD, Chen, JM, ''Marvelous Abilities for Polyhedral Oligomeric Silsesquioxane to Improve Tribological Properties of Polyamide-Imide/Polytetrafluoroethylene Coatings.'' *J. Mater. Sci.*, **53** (17) 12616–12627 (2018)
33. Wang, X, Hu, Y, Song, L, Xing, W, Lu, H, Lv, P, Jie, GX, ''UV-Curable Waterborne Polyurethane Acrylate Modified with Octavinyl POSS for Weatherable Coating Applications.'' *J. Polym. Res.*, **18** 721–729 (2011)
34. Godnjavec, J, Znoj, B, Veronovski, N, Venturini, P, ''Polyhedral Oligomeric Silsesquioxanes as Titanium Dioxide Surface Modifiers for Transparent Acrylic UV Blocking Hybrid Coating.'' *Prog. Org. Coat.*, **74** 654–659 (2012)
35. Li, H, Zhao, X, Chu, G, Zhang, S, Yuan, X, ''One Step Fabrication of Superhydrophobic Polymer Surface from an Acrylic Copolymer Containing POSS by Spraying.'' *RSC Adv.*, **4** 62694–62697 (2014)
36. Huang, XX, Liao, WB, Ye, LY, Zhang, N, Lan, SH, Fan, HB, Qu, JQ, ''Fabrication of Hydrophobic Composite Films by Sol-Gel Process Between POSS-Containing Fluorinated Polyacrylate Latexes and Colloidal Silica Particles.'' *Micropor. Mesopor. Mater.*, **243** 311–318 (2017)
37. Cordes, DB, Lickiss, PD, Rataboul, F, ''Recent Developments in the Chemistry of Cubic Polyhedral Oligosilsesquioxanes.'' *Chem. Rev.*, **110** 2081–2173 (2010)
38. Chen, D, Yi, S, Wu, W, Zhong, Y, Liao, J, Huang, C, Shi, WJ, ''Synthesis and Characterization of Novel Room Temperature Vulcanized (RTV) Silicone Rubbers Using Vinyl-POSS Derivatives as Cross Linking Agents.'' *Polymer*, **51** 3867–3878 (2010)
39. Wang, W, Jie, X, Fei, M, Jiang, H, ''Synthesis of Core-Shell Particles by Batch Emulsion Polymerization of Styrene and Octavinyl Polyhedral Oligomeric Silsesquioxane.'' *J. Polym. Res.*, **18** 13–17 (2011)
40. Baney, RH, Itoh, M, Sakakibara, A, Suzuki, T, ''Silsesquioxanes.'' *Chem. Rev.*, **95** 1409–1430 (1995)
41. Li, G, Wang, L, Ni, H, et al., ''Polyhedral Oligomeric Silsesquioxane (POSS) Polymers and Copolymers: A Review.'' *J. Inorg. Organomet. Polym.*, **11** (3) 123–154 (2001)
42. Ke, F, Zhang, C, Guang, S, Xu, H, Xu, HY, ''POSS Core Star-Shape Molecular Hybrid Materials: Effect of the Chain Length and POSS Content on Dielectric Properties.'' *J. Appl. Polym. Sci.*, **127** 2628–2634 (2013)
43. Yang, B, Li, J, Wang, J, Xu, H, Guang, S, Li, C, ''Poly(vinyl Pyrrolidone-Co-Octavinyl Polyhedral Oligomeric Silsesquioxane) Hybrid Nanocomposites: Preparation, Thermal Properties, and Tg Improvement Mechanism.'' *J. Appl. Polym. Sci.*, **106** (1) 320–326 (2010)
44. Yang, B, Li, J, Wang, J, et al., ''Poly(vinyl Pyrrolidone-Co-Octavinyl Polyhedral Oligomeric Silsesquioxane) Hybrid Nanocomposites: Preparation, Thermal Properties, and T_g Improvement Mechanism.'' *J. Appl. Polym. Sci.*, **111** (6) 2963–2969 (2009)
45. Xu, H, Yang, B, Wang, J, Guang, S, Li, C, ''Preparation, Tg Improvement, and Thermal Stability Enhancement Mechanism of Soluble Poly(methyl Methacrylate) Nanocomposites by Incorporating Octavinyl Polyhedral Oligomeric Silsesquioxanes.'' *J. Polym. Sci. Polym. Chem.*, **45** 5308–5317 (2010)